



Sketching a Space of Brain States

Maria Mannone^{1,2,3,5} · Patrizia Ribino¹ · Peppino Fazio^{3,4} · Norbert Marwan^{2,5,6}

Accepted: 14 July 2025
© The Author(s) 2025

Abstract

Brain functional connectivity alterations, that is, pathological changes in the signal exchange between areas of the brain, are occurring in several neurological diseases, including neurodegenerative and neuropsychiatric ones. They consist in changes in how brain functional networks work. By conceptualising a brain space as a space whose points are connectome configurations representing brain functional states, changes in brain network functionality can be represented by paths between these points. Paths from a healthy state to a diseased one, or between diseased states as instances of disease progression, are modelled as the action of the *Krankheit-Operator*, that produces changes from a brain functional state to another one. This study proposes a formal representation of the space of brain states and presents its computational definition. Moreover, references to patients affected by Parkinson's disease, schizophrenia, and Alzheimer-Perusini's disease are included for discussing the proposed approach and possible developments of the research toward a generalisation.

Keywords Phase space · Brain network · Connectome · *K*-operator

Introduction

Mind wandering can be a poetic image. What about a multi-dimensional space where brains can actually move through? A space whose points are *brain states*. Let us gradually introduce the idea, starting from a construction for each brain, the *connectome* (Sporns & Tononi, 2005; Hagmann, 2005). It

is a graph-like representation of the most active brain areas, indicated as nodes (often indicated as *hubs* (van den Heuvel & Sporns, 2013)), and connected through links (see Fig. 1).

Structural connectivity is investigated via tractography (Smith et al., 2012), whose starting point is the anisotropy of diffusion of water molecules, and functional connectivity via functional magnetic resonance (Buxton, 2013), whose starting point is the alteration of blood circulation to replenish oxygen to the most active brain areas, at rest, or during a given task.

Seeing the brain as an instance of complex networks (Newman, 2003; Battiston et al., 2020), the alterations of the connections can be related to diseases. This is widely investigated through data analysis in studies dealing with the alteration of connectivity in neurological disorders. Examples range from disconnection syndrome (Schummer, 2009), to schizophrenia (van den Heuvel et al., 2010), to neurodegenerative disorders, such as Alzheimer-Perusini's disease (Staff, 2022; Fathian et al., 2022) and Parkinson's disease (Bergamino et al., 2023; Sang et al., 2015), especially including functional connectivity (Mosley & Robinson, 2023; Morris et al., 2023; O'Shea et al., 2022; Blandini et al., 2000).

In an attempt to generalise the approach to neurological disease and pave the way towards integrated systems for healing, as desired in Seeley (2017), a formalism joining matrix algebra, a physics-like approach with operators acting on

✉ Maria Mannone
maria.mannone@uni-potsdam.de

Patrizia Ribino
patrizia.ribino@icar.cnr.it

Peppino Fazio
peppino.-fazio@unive.it

Norbert Marwan
marwan@pik-potsdam.de

¹ ICAR, National Research Council (CNR), Palermo, Italy

² Institute of Physics and Astronomy, University of Potsdam, Potsdam, Germany

³ DSMN, Ca' Foscari University of Venice, Venice, Italy

⁴ VSB, Technical University of Ostrava, Ostrava, Czechia

⁵ Potsdam Institute for Climate Impact Research (PIK), Member of the Leibniz Association, Potsdam, Germany

⁶ Institute of Geosciences, University of Potsdam, Potsdam, Germany

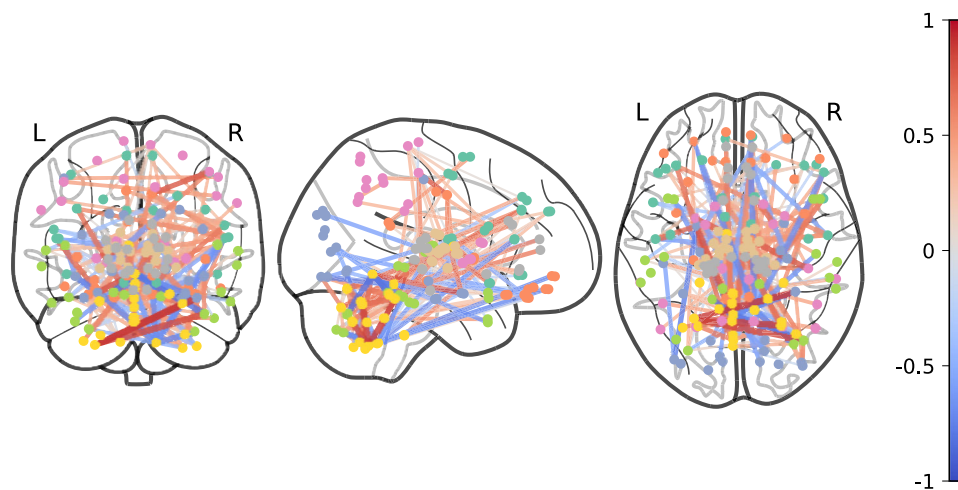


Fig. 1 Different perspectives of a human connectome

observables, and real-data analysis, the *Krankheit*-Operator (from German *disease*, in short *K*-operator), has been proposed (Mannone et al., 2024b). Specific forms of the operator represent the key features of specific neuropsychiatric and neurodegenerative diseases.

As a further step in the abstraction, we can imagine a space of connectomes, where each connectome is a point, and the transformations between them are paths. While several studies investigate how space can be represented within the human brain (Buzsáki & Llinás, 2017), we are interested in finding how a brain can be represented within a conceptual space, as a parameter space. The closer attempt to such an endeavour was proposed in Fard and Ragan (2017). The authors, drawing upon Waddington's epigenetic landscape for cell development, propose a Hopfield network formalism to build up an attractor model of disease progression based on networks of proteins or genetic correlation. Disease progression is modelled through the reference to curves within a space, where each point is a specific network configuration; however, the focus is more on genetics (Fard & Ragan, 2017). Normal state and diseased states are space regions considered as attractors. In their 3D representation, the axes contain the first principal component, the second principal component, and the energy. The presented examples include Parkinson's disease, glioma, and colon cancer.

Our representation, developed independently from this study, also contains states within a space and subspaces for healthy and diseased states, but it is built in a completely different way, considering the brain connectome and encoding information on brain areas into the three axes. As another difference, we shift the attention from attractors within the space to the operator leading time evolution, in particular, considering disease time evolution, that is, the *K*-operator (Mannone et al., 2024b). Other studies focus on brain diseases, seeing them as attractors (Seraji et al., 2024).

In this article, inspired by the phase space theory (Reichl, 1998) where the set of all possible physical states of a system corresponds uniquely to points in the phase space, we propose a Brain Space where points represent specific brain states and whose paths are the transitions from a brain state to another one, as mappings between them. Choosing to describe a brain as its connectome, the points of the space are specific connectomic configurations, and the paths are transformations of connectomes, i.e., changes in brain-network functionality.

Before moving forwards, we present in Table 1 a little glossary of the most used acronyms in this paper.

Our proposed approach is theoretical, and the selected case studies are used here to illustrate the method. They are not exhaustive, but they help instantiate the definitions, define the methodology, the advantages, and the limitations.

The rest of the paper is organised as follows. We sketch our theoretical idea in Section 2, and we propose a possi-

Table 1 Table with the most used acronyms in this article

Acronym	Complete Name
fMRI	Functional magnetic resonance imaging
DICOM	Digital Imaging and Communications in Medicine
NIFTI	Neuroimaging Informatics Technology Initiative
ROI	Region of Interest (of the brain)
ADNI	Alzheimer's Disease Neuroimaging Initiative
PPMI	Parkinson's Progression Markers Initiative
COBRE	Center for Biomedical Research Excellence
FU	Follow-Up
AD	Alzheimer(-Perusini)'s disease
PD	Parkinson's disease
thal_MGN_R	Medial Geniculate Right
thal_LGN_R	Lateral Geniculate Right

ble implementation of it in Fig. 3, discussing the results in Section 4. Possible research developments are listed in the Conclusions.

Theoretical View

We propose a **Brain Space as a phase space**, where each point is a connectomic state. But we know that each brain is in itself a nested network, from neurons, to neuronal agglomerates, to the connectome (Fig. 2). A transformation of the connectome over time is a path between points in the Brain Space. The size of the connectome depends upon the chosen number of nodes, that is, the number of regions of interest (ROIs) the brain can be divided into. A brain atlas (Tzourio-Mazoyer et al., 2002; Varoquaux et al., 2011; Kennedy et al., 2023) defines the shape and location of brain regions in a common coordinate space. Hence, the degree of resolution of brain analysis influences the choice of brain atlas: the more the regions of interest, the higher the number of points of the connectome.

Let N be the number of ROIs in a chosen atlas and let us consider retaining all information, then the number of degrees of freedom in our brain space will be N . From phase space theory if we consider all possible values of the *position*

(i.e., the state in which a brain is) and *momentum* (i.e., the movement from one state to another one), then the number of degrees of freedom doubles to $2N$, resulting in a $2N$ -dimension brain space.

What are *position* and *momentum* for the connectome? Since a connectome is a dynamical model, the position indicates where a connectome is at time t , and the momentum determines how it is changing from one state to another.

The transition from one state to another is a normal process due to learning (with the consequent development of brain areas), feeling emotions, or ageing. A normal time evolution is described with paths within the “healthy states” subspace, see the bottom right side of Fig. 2, where the “healthy evolution” brings a brain of a person generically indicated as A, in a healthy state $\mathcal{G}_{A,i}$, towards another healthy state $\mathcal{G}_{A,j}$.

On the other hand, abnormal dynamical processes concern the transitions under the effect of functional neurologic disorder onset, or exceptionally overwhelming emotions or trauma. A brain point can move towards states outside the healthy-state subspace, reaching a diseased state; see the path for the brain of a generic patient A toward $\mathcal{G}_{A,j}^k$, under the effect of the action of K , on the right side of Fig. 2.

In fact, such a process develops under the action of K (see Fig. 3), modelled as an operator altering the weights of links in the connectome, reproducing the onset or progression of

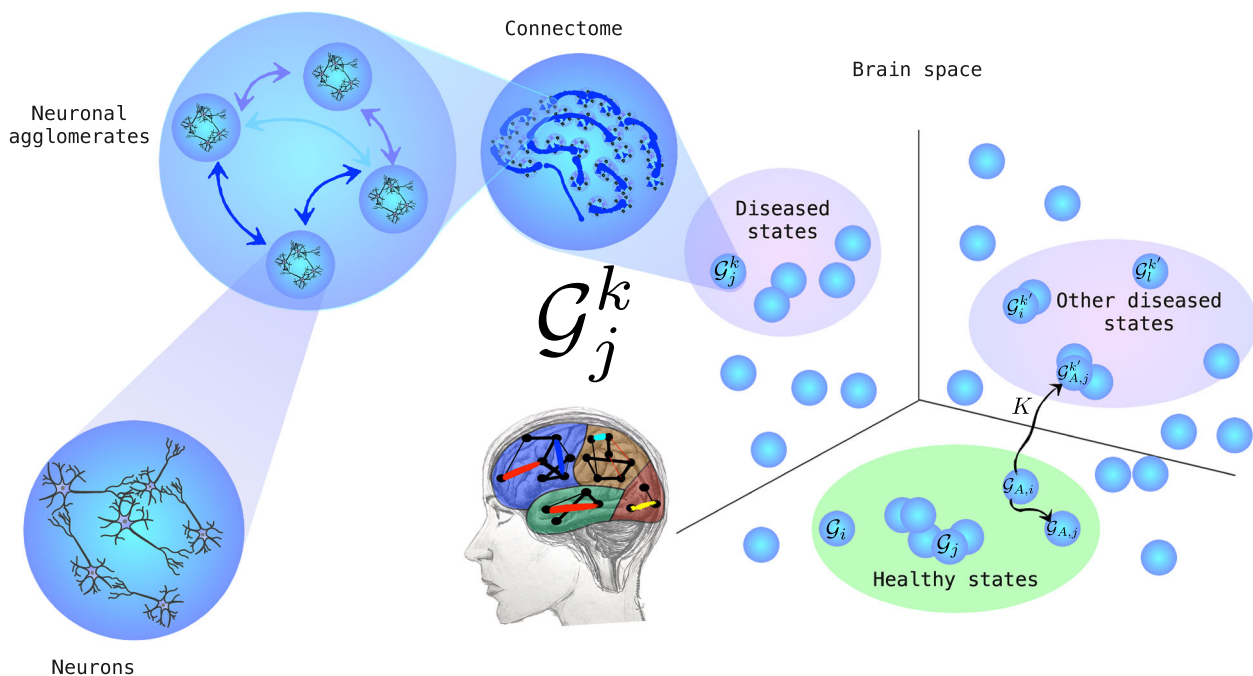


Fig. 2 Left: pictorial representation of the brain as a nested network, from neurons, to neuronal agglomerates, to the connectome. Right: Space of brain states, where each connectome is a point, and the transformation of a specific brain over time can be represented as a path from one state to another. Bottom right: the path from a brain of person

A from state $\mathcal{G}_{A,i}$ to state $\mathcal{G}_{A,j}$ lies within the healthy states, while the pathological evolution brings the brain towards the state $\mathcal{G}_{A,j}^k$ within one of the diseased states’ subspaces. (Drawing and graphics by Maria Mannone)

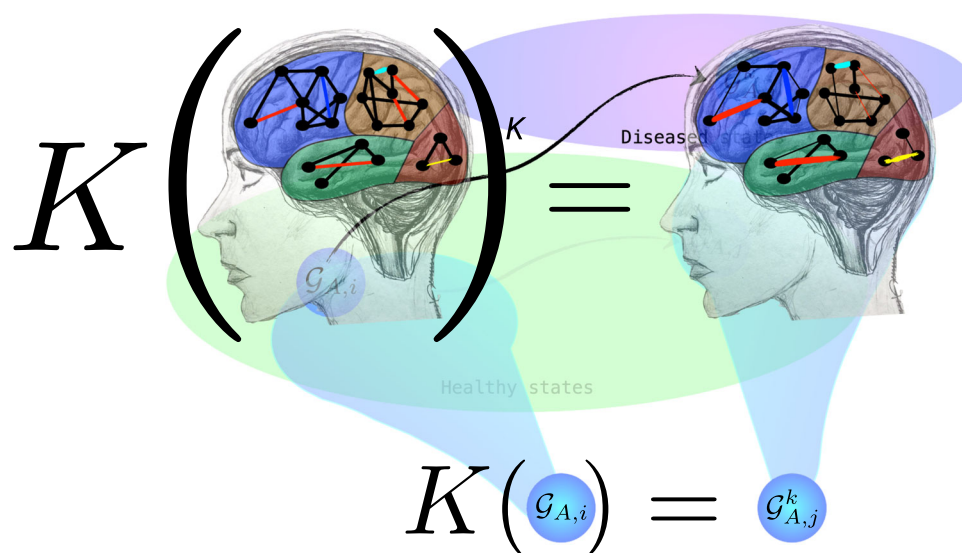


Fig. 3 Pictorial representation of the K -operator on a brain. Drawing by Maria Mannone

specific neurological disorders (Mannone et al., 2024b, c), as in Eq. 1:

$$K(t)\mathcal{G}^k(t) = \mathcal{G}^k(t+1). \quad (1)$$

In Eq. 1, K may act on a healthy connectome leading to a diseased one or on an already-diseased brain, letting the disease worsen. Hence, the action of K leads a brain along a path within subspaces of specific diseases or brings a brain out of the healthy subspace or even back and forth, as in epilepsy or mood disorders. Thus, the paths in the brain space are governed by “simple dynamics” if the states and the paths between them remain within the healthy subspace. That is, the brain dynamics can keep the states of a brain gravitate within a basin of attraction. The precise shape of the dynamics depends upon the changes of the brain: normal ageing, continuous learning, new skills development all contribute to the shaping of the brain and functional connectivity. While also the anatomic connectivity is affected by pathological and, up to a certain extent, also by normal processes (as learning how to play a musical instrument), in this study we focus on the functional one. An ideal “normal state” considering age range can be treated as a probabilistic attractor, towards which the brain states gravitate to. If more disorders are present in the same patient, the matrix elements of the K -operator for these disorders are also involved. A precise discrimination can be performed when we compare the K obtained from patients with comorbidities with this K s obtained from patients affected by only one of these diseases.

The paths are governed by the K -operator if the states are outside or moving from the healthy subset to the outside. A process bringing a brain back to the healthy subspace is a healing process. The ideal healing is the inverse of the K -

operator: K^{-1} . A sequence of healing steps for a progressive healing process is described by Mannone et al. (2024a), as well as the definition of a *missing therapy* from the ideal healing and the already-existing, partial healing strategies.

The K -operator is a nonlinear operator, but some linear approximations have been proposed. It is time-dependent; in Mannone et al. (2024b), a precise functional, t-dependent shape of the operator was proposed for its elements after the characteristics of some specific disorders. In other studies (Mannone et al., 2024c), only specific numerical forms of the K -operators have been computed, between two time points.

The key idea is the theoretical definition of a space of brain states. The use of multi-dimensional scaling (MDS), that will be discussed later, is only a possible way to compress the information concerning the ROIs. Thus, MDS is only instrumental. The key point is the definition of a conceptual framework to represent the transformation of brain states over time, both within the healthy domain, and between healthy and pathological states, which is characteristic of diseases such as epilepsy or bipolar disorders. The K -operator is a novel idea that starts being developed. Our wish is that it can also be further adopted and explored by different researchers. However, in this study, the concept of K is merely used as label for the trajectory of a brain across states including diseased states, that is, to characterise its pathological time evolution.

Summarizing, we can state that **a brain is healthy if all its states throughout time remain within the healthy states subspace in a stable way. A diseased brain heals if its states move from the disease’s subspaces towards the healthy states’ subspace and then remain there stably.** Remaining within the healthy-state subspace does not mean that the brain is not changing: it means that it changes in a

normal, non-pathological way. It is the case of the growing process, from childhood to adulthood, and progressively with healthy ageing. Also learning shapes the brain, strengthening some connections and enlarging some brain areas. A classic example is constituted by the brain changes in musicians (Olszewska et al., 2021; Sacks, 2007). Thus, they impact both the anatomic connectivity, as well as the functional connectivity.

A Two-stage Approach to Compute a Brain Space

Here, we describe the two-stage approach to compute the Brain Space. The first stage allows for obtaining a single brain state points of the space starting from the fMRI images, while the second one allows for the construction of the whole brain space.

As said before, the points of the proposed brain space are connectomes. By focusing on fMRI-derived data from some real patients, we obtain connectomes as a connectivity matrix for each brain according to the steps described in the following pseudocode¹.

Algorithm 1 Brain states computation.

Data: fMRIs as DICOM files

Result: Brain Space points

Step 1: fMRI conversion

Convert the DICOM files to NIfTI format;

Step 2: Atlas selection

Choose a medical atlas to be used as a mask to group matrix elements of NIfTI within specific brain areas;

Step 3: Time series extraction

Extract time series for each ROI;

Step 4: Connectivity matrix computation

Compute the connectivity matrix as a correlation matrix, whose elements are the correlation values between pairs of ROIs averaged over time;

Step 5: Matrix labelling

Label each matrix as $\mathcal{G}_j^k(t)$ for disease k and patient j at the time visit t .

For instance, the brain matrix of a patient at the first visit and the brain matrix of the same patient at the first follow-up will be two different points in the space of brains, and the transition from baseline to follow-up will be a path in the brain space between these two points. However, no absolute time is considered: e.g., the brain state of another patient,

¹ In this paper, we used the Pearson correlation. However, other correlation methods can be used.

whose baseline measure was obtained six months before the baseline of the first patient, will just be another point in the space. In this way, we obtain the single points of our brain space, and that will be used to compute the values on the axes via a *multi-dimensional scaling* (MDS) as described in the following. The technique to compute MDS is standard, however here the novelty is represented by the overall framework of brain spaces, and by the meaning of dimensions in this study. The MDS dimensions are orthogonal, and they are computed as the weighted sum of the 160 regions of interest (ROIs) of the human brain for which all the considered brain matrices are non-empty. The weights are computed according to the impact of the Frobenius distance between corresponding elements of the matrices representing functional brain connectivity in each considered brain state. The higher the weight, the more important a pair of ROIs is for distinguishing between different brain states. The correlation of a single ROI to the axis takes into account its relative impact on the different pairs, as it will be further explained later.

Let us now describe how a brain space can be obtained, how we can shape it as a 3D shape for visualisation, and what meaning can be assigned to the axes. Through the MDS algorithm, arbitrarily selecting 3 as the number of dimensions, we can automatically arrange the matrix points in the space. The closer the points, the more similar the matrices (and thus the corresponding brain states). To this aim, here we consider element-wise similarity (with Euclidean distance) of the matrices. In particular, concerning the distance metric, we finally decided to focus on the Frobenius distance. The main steps to represent the brain space are illustrated in the following pseudocode.

Algorithm 2 Brain space representation.

Data: $\mathcal{G}_j^k(t)$ for disease k and patient j at the time visit t

Result: 3D visualization of Brain Space

Step 1: ROI selection

Step 2: Space points distribution

Distribute space points according to element-wise similarity;

Step 3: MDS scaling

Perform multi-dimensional scaling according to the space dimension;

Step 4: Axes value computation

Compute the values of the axes as contributions of the ROI with weights automatically chosen according to the inputted brains;

Step 5: Plotting

Plot the Brain Space;

Step 6: ROI contribution

Print list of the ROIs and their correlation to each axis;

Step 7: Better ROIs selection

Finding which ROIs help better differentiate between brain states.

Table 2 List of patients in Figs. 4 and 5

label	disease	ID patient	time	age	sex	dataset
AD	AD	002_S_5018 (Mannone et al., 2025)	baseline	73	male	ADNI 2
PD	PD	100878 (Mannone et al., 2024c)	baseline	67	male	PPMI
schizo	schizophrenia	sub-A00015518 (Mannone et al., 2024c)	baseline	60	male	COBRE
normal	–	101195 (Mannone et al., 2024c)	baseline	74	male	PPMI
AD_fem	AD	019_S_5019 (Mannone et al., 2025)	baseline	63	female	ADNI 2
AD_fem_FU	AD	019_S_5019 (Mannone et al., 2025)	follow-up	63	female	ADNI 2
AD_patC	AD	006_S_4153 (Mannone et al., 2025)	baseline	79	male	ADNI 2
AD_patC_FU	AD	006_S_4153 (Mannone et al., 2025)	follow-up	79	male	ADNI 2
PD_patB	PD	100006 (Mannone et al., 2024c)	baseline	56	female	PPMI
PD_patB_FU	PD	100006 (Mannone et al., 2024c)	follow-up	56	female	PPMI
normal_F	–	018_S_4399 (Mannone et al., 2025)	baseline	78	female	ADNI 2
PD patient*	PD	101050	baseline	50	female	PPMI

(* is not present in Fig. 4, but was included in Fig. 5). AD stands for Alzheimer-Perusini's disease, PD for Parkinson's disease. The references indicate preliminary studies on the K -operator where these patients have been considered

No ROIs were removed as uninformative; the only regions actually removed are those missing from one or more matrices of the selected brains. But this step was preliminary to the overall analysis, and thus 160 ROIs out of 170 ROIs in the Anatomic Automatic Labeling 3 (AAL3) atlas were considered. Finally, we provide the details for performing the MDS in step 4. For each axis, MDS performs a weighted sum of the ROIs, where the most influential ones have higher weight (that is, higher correlation as an absolute value with the axis).

Algorithm 3 Projection of 3D Matrices according to their similarity.

Data: Matrix of distances D , labels L , names of the matrices N , dictionary of visualised indices S

Result: Interactive 3D visualization of matrices

Step 1: MDS projection

Run MDS on D to get a 3D representation \mathbf{P} ;

Step 2: initialization of the 3D graph

Create a new empty 3D figure fig ;

Step 3: addition of matrices to the graph

Add to fig a scatter plot 3D, by using \mathbf{P} , with labels N and colours based on L ;

Step 4: addition of complex hulls for selected groups

if $S \neq \emptyset$ then

 assign a list of distinct colours C ;

foreach group g in S **do**

 select points \mathbf{P}_g corresponding to g ;

 compute the complex hull H_g of \mathbf{P}_g ;

 extract vertices V_g of H_g ;

 add to fig a mesh 3D for H_g with colour from C ;

 add to fig a scatter plot 3D for the points in g

 with colour from C .

end

end

Experimental Results

In this section, we provide a computation of a Brain Space obtained from a set of patients. In particular, to highlight differences between brain functional alterations due to different diseases, we choose patients from different healthcare datasets relating to different neurological disorders as listed in Table 2. We chose states of patients with healthy brains or with diseased brain, with features representative of the respective disorders. In particular, we focus on patients individually investigated for preliminary applications of the K -operator for specific disorders. Moreover, we chose the Anatomic Automatic Labeling 3 (AAL3) atlas (Rolls et al., 2020) and selected the 160 ROIs within all the fMRIs of the considered patients.

In Fig. 4, we can see the Brain Space generated for the patients in Table 2.

On the other hand, Fig. 5 shows the simplex (violet) of Alzheimer-Perusini's patients and the simplex (blue) of Parkinson's patients. As we can see, there is a clear separation between these disease subspaces.

As concerns the schizophrenic patient, he is distant from the PD patients and even more distant from the follow-up of one of the PD patients. This makes sense since the evolution of PD involves a defect of dopamine neurotransmitters due to damage in the substantia nigra, and a consequent deficit in dopamine is "opposed" to the excess of dopamine occurring in the same region for schizophrenic patients (van Hooijdonk et al., 2023).²

² Pathways of dopamine are disrupted in different ways in schizophrenic brains. According to some authors, the excessive dopamine activity in the mesolimbic neurons is caused by an abnor-

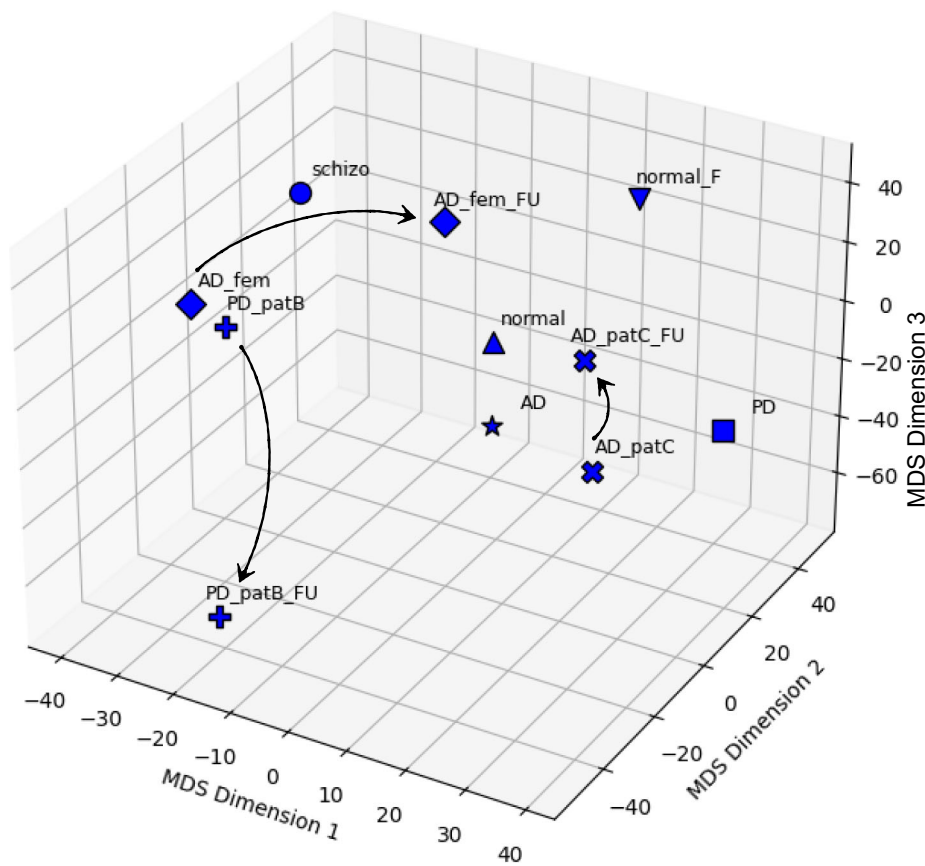


Fig. 4 A quantitative example of brain space for a selection of patients. For the explanation of the points’ labels, see Table 2 (right). The labels contain a weighted sum of the regions of interest, automatically com-

puted (Table 3). The states belonging to the same patients are identified with the same symbol. The arrows, indicating time evolution, are added as post-processing

The axes of Figs. 4 and 5 contain the synthetic description of MDS dimensions 1, 2, and 3. The MDS algorithm automatically computes a weighted sum of the contribution of each region of interest for each axis in terms of correlation values. The higher the ROI absolute value, the higher the impact of the ROI in the space separation between points.

It is worth noting that MDS is a dimension-reduction technique designed to project high-dimensional data down to lower dimensions while preserving relative distances between observations. Since in our example we reduce 160 ROIs to obtain a 3D representation of the Brain Space, the more points we add to the Brain Space, the more the axes values are refined.

Table 3 shows the first five more impacting ROIs on each axis, before (left) and after (right) the addition of the last patient of Table 2. With a larger population, the classification could become more precise. Nevertheless, with this simple example, we also draw information on the feasibility of

our brain state definition from a purely theoretical approach to a computational one.

The MDS are computed after the pairs of ROIs, the most influential to distinguish between brain states according to the \mathcal{G} matrices. They can also be related to the single ROIs most influential in those pair variations. Our reported ROI correlations are still exploratory, but the analysis can be enriched with the features directly derived from the connectivity matrices. In fact, the individual impact of ROIs on an MDS axis is obtained via the sum of the contributions of all connections involving that ROI. And it includes a 1/2 factor, to avoid counting a pair of ROIs twice. By considering the impact of the “original” pairs of ROIs, we can listen the first of them according to their impact, as shown in Table 4, directly for the case study with all patients.

The MDS distribution is sensitive to the characteristics of inputted brain states. In fact, a progressive refinement can be achieved with the addition of more patients.

To complete the discussion of the brain space, we also give a quantitative representation of a path. Within the brain space, the progression of the disease is an arrow, labelled as

ally low prefrontal dopamine activity, leading to cognitive symptoms (Davis et al., 1991).

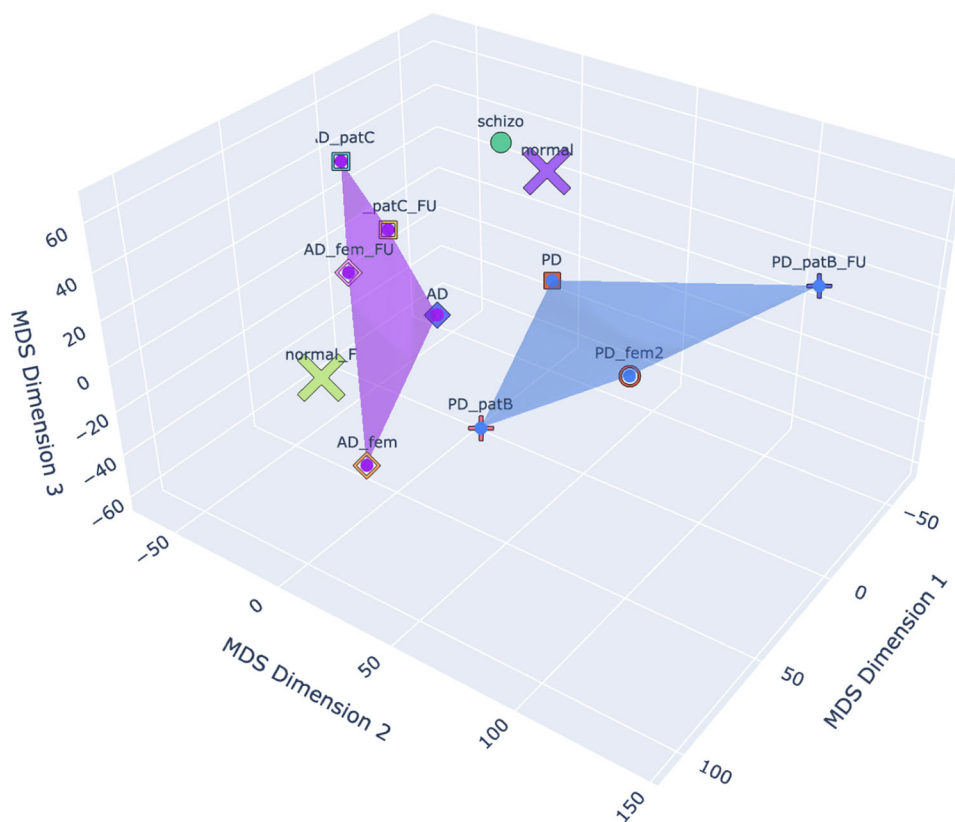


Fig. 5 A quantitative example of brain space for the selected patients, where we also use the same symbol for the same patient, with the exception of the two normal ones, with the same symbol, an × (limitation of the available marker shapes in 3D in Python). Here: Euclidean dissimilarity

Table 3 The first five ROIs more heavily affecting (in absolute value) the axis content of the brain space, before (left) and after (right) the inclusion of the last patient in Table 2

ROI	correlation	ROI name	ROI	correlation	ROI name
Dimension 1 (axis x)					
71	0.739	Precuneus_L	60	0.702	fusiform_R
30	-0.724	OFCpost_R	72	0.696	precuneus_R
16	0.724	Supp_Motor_Area_R	66	0.688	parietal_inf_R
66	0.688	parietal_inf_R	2	0.685	precentral_R
64	0.719	Parietal_Sup_R	140	0.680	thal_LGN_R
Dimension 2 (axis y)					
102	0.866	Cerebellum_4_5_R	20	0.868	frontal_superior_med_R
84	0.833	Heschl_R	14	0.838	rolandic_oper_R
56	0.794	Occipital_Mid_R	66	0.835	parietal_inf_R
86	0.750	Temporal_Sup_R	10	0.830	frontal_inf_tri_R
10	0.738	Frontal_Inf_Tri_R	6	0.824	frontal_mid_2_R
Dimension 3 (axis z)					
106	-0.877	Cerebellum_7b_R	142	0.824	thal_MGN_R
91	-0.875	Temporal_Pole_Mid_L	89	-0.804	temporal_mid_L
89	-0.837	Temporal_Mid_L	91	-0.800	temporal_pole_mid_L
85	-0.820	Temporal_Sup_L	106	-0.798	cerebellum_7_R
99	-0.809	Cerebellum_3_L	55	-0.794	occipital_mid_L

Table 4 The most influential pairs of ROIs

1st ROI	2nd ROI	Variance
115	116	0.33
74	78	0.33
114	116	0.32
46	70	0.31
104	115	0.30
49	70	0.30
113	116	0.30
106	115	0.30
98	116	0.29
57	86	0.29
45	70	0.29
61	99	0.29
100	116	0.29
105	116	0.29
151	152	0.28
104	116	0.28
99	115	0.28
61	106	0.28
57	115	0.28
46	61	0.28

The bold indicates the ROIs also present in the list of the first five most influential individual ROIs in each axes, or very close ones

the *K*-operator, transforming, for instance, the brain state of a Parkinsonian patient at the baseline (for example, PD_patB) to the state at the first follow-up (for example PD_patB_FU). If we consider a space of a number of dimensions equal to the number of ROIs, thus 160 in the present case, then the brain-state path from baseline to follow-up is perfectly described by the *K*-operator computed between the two states and for that choice of atlas. However, in these compressed dimensions via a multi-dimensional scaling, some ROIs will contribute more than others, depending on the other states in space, see Table 2. Then, the path under consideration will be described by a compressed version of the *K*-operator. By extracting the coordinates of the points PD_patB and PD_patB_FU, we can write:

$$K_{\text{space MDS, 3D}} : PD_patB \rightarrow PD_patB_FU \tag{2}$$

$$\Rightarrow [-34.25, -15.81, -3.611] \rightarrow [-13.48, -47.21, -69.99].$$

Hence the **path from PD_patB to PD_patB_FU can be computed as the percentage of variation of each of these ROIs**. For the MDS Dimension 1 we have 60.64%, for Dimension 2 we have 198.61%, and finally for Dimension 3 we get 1838.24%. These percentage variations have to be reported on the five most influential ROIs and their correlation with the axes from Table 3. Limiting ourselves to the

first ROIs for each axis, we can assess that the strongest alteration occurs for the third MDS dimension, and thus mostly impacting the first ROI of the list, cerebellum 7b right or the thalamus geniculate (considering the left or right side of Table 3), followed at large by the second MDS dimension with cerebellum 4R or frontal superior medial R, and the first MDS dimension, whose greater weight is constituted by precuneus left or fusiform right. However, due to the two orders of magnitude of the change in the third MDS dimension, also the other four ROIs that are impacting that axis are worthy of notice (temporal mid-left, temporal pole mid-left, cerebellum 7 right, and occipital mid-L).

By looking at Fig. 6 taken from (Mannone et al., 2024c) representing the *K*-operator for the disease progression of patient B and highlighting the mentioned regions (with thicker lines for the first ROIs of the third dimension), we check that they correspond to specific clusters of (mostly blue, i.e., negative) points in the *K*-operator for the 160 ROIs.

We can relate the coordinates of the two brain states connected by the considered *K*-operator to the most influential pairs of ROIs. In particular, we can focus on the third axis, the one where the higher change is found. We thus obtain the list of Table 5. In particular, we notice the pairs:

- 15-87 supplementary motor area, and temporal pole: superior temporal gyrus;
- 5-6, both middle frontal gyrus;
- 27-87 anterior orbital gyrus, and temporal pole: superior medial frontal gyrus,

and in particular the ROIs:

- 3: superior frontal gyrus,
- 35: anterior cingulate,
- 1: precentral gyrus,
- 37: middle cingulate gyrus,
- 84: Heschl’s gyrus,
- 70: angular.

From the evaluation of the complete *K*-operator (Figure 6), we can notice the impact of the nearby pairs of ROIs 89-21, 90-21, near to 15-87 and 27-87, and we can also notice, from visual inspection, the importance of the agglomerates around 5-6, and the small agglomerates in correspondence of 71-35. The highlighted areas, near to the regions of Table 5, are the following:

- 89: middle temporal gyrus,
- 21: superior frontal gyrus,
- 27: anterior orbital gyrus,
- 71: precuneus, and
- 35: anterior cingulate.

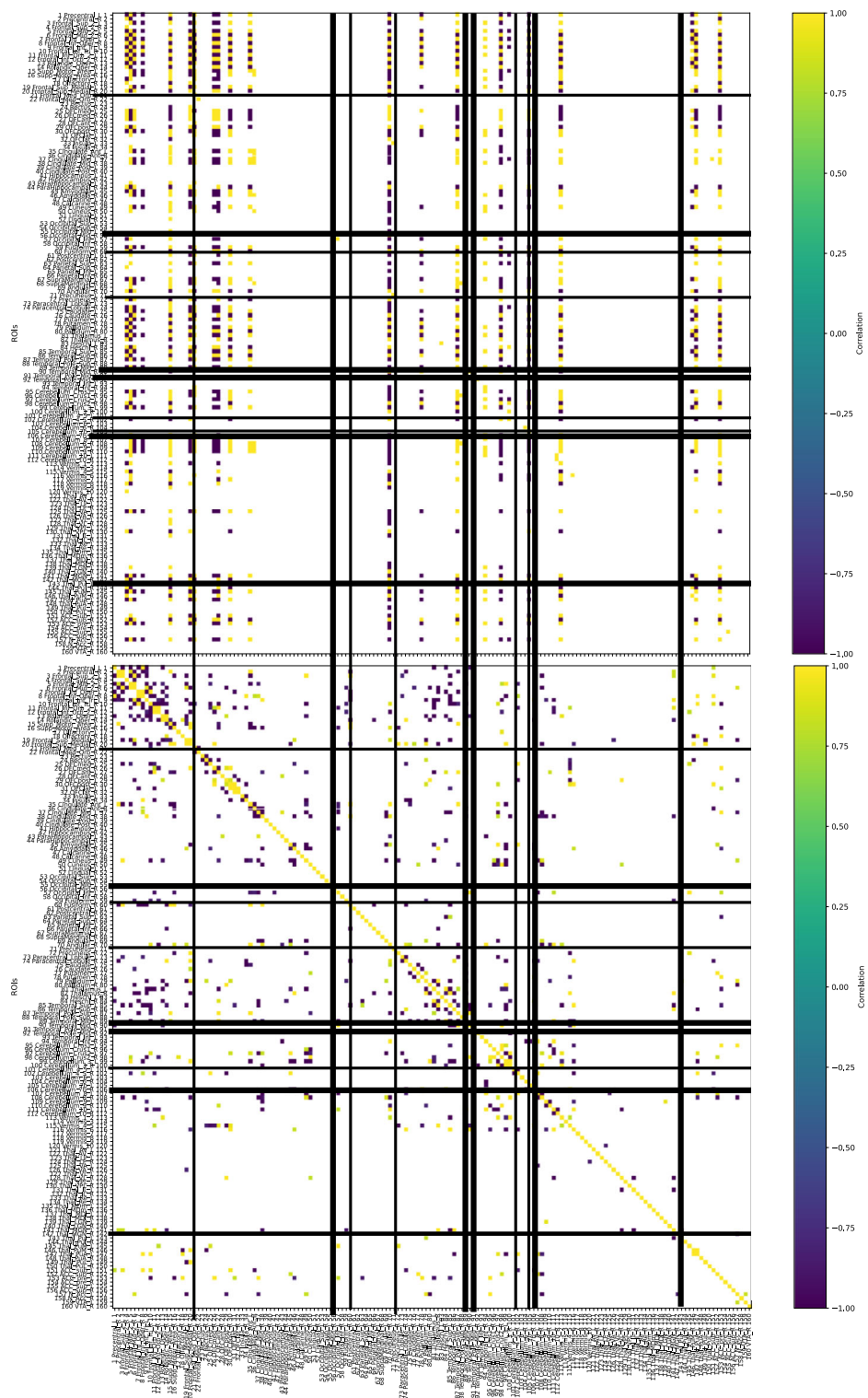


Fig. 6 K -operator for the disease progression of patient B (Table 2), from the baseline to the first follow-up. The thicker lines indicate the first ROIs more correlated with the third MDS dimension, where the change from baseline to follow-up is higher. (Original figure taken from (Mannone et al., 2024c))

Table 5 The most influential pairs of ROIs concerning the third axis, MDS dimension 3, where the higher change is highlighted for the considered example (patB, from baseline to the first follow-up)

ROI-ROI pair	connectivity change	axis estimated contribution
15 - 87	1.78	-1.549
5 - 6	-1.76	1.535
27 - 87	-1.74	1.517
3 - 6	-1.74	1.511
6 - 35	-1.71	1.489
1 - 87	1.71	-1.485
6 - 37	-1.71	1.484
84 - 87	-1.70	1.483
35 - 87	1.70	-1.481
37 - 70	-1.70	1.478

The values in the last column decrease (in absolute value) from the first to the last column. This is more evident if more pairs are printed

Summarising, the “classic” strategy for the computation of the K -operator is: ROIs \rightarrow \mathcal{G} -matrices \rightarrow K -operator (without dimensional loss), while the strategy proposed in this article, to provide a computational example of construction of brain spaces, is: ROIs \rightarrow MDS \rightarrow positioning of \mathcal{G} s as points in the brain space, and subsequently the computation of the K -operator within the reduced space.

Conclusions

In this article, we introduced the concept of brain spaces, where each point is the connectivity matrix of a connectome. The closer the points within the space, the more similar the connectomic configurations between them. Such a representation allows a quantitative analysis of similarity and dissimilarity between brains in states corresponding to specific diseases, or oscillating behaviours between healthy and diseased states, as in the case of mood disorders or epilepsy. We also quantitatively defined a path connecting two points of the space, relating it to the variation of connectivity between pairs of brain regions. In particular, the path from a healthy state to a diseased one, or between two diseased states as a disease progression, is the result of the action of the K -operator, recently proposed as a mathematical operator reproducing the key features of a disease, modifying the weights of the connections between brain regions. In this research, we chose to focus on functional connectivity, and thus the functional magnetic resonance imaging was adopted as the original source of our data. Future investigations will also include tractography, for a precise information

on the anatomic alterations of the brain cortex. In fact, a more comprehensive investigation will also include a comparison between functional and anatomic alterations.

Possible research developments concern an extension of the operator, including neurotransmitters, neurochemistry, and other biomarkers. This would allow a more comprehensive representation of the operator, as its action on different levels of the brain, and of other parameters influencing the brain states. Considering the healing process as the inverse of disease progression (Mannone et al., 2024a), an action on de-inflammation and neurochemistry can have a decisive role in the connectomic healing.

To generalise the K -operator including other parameters, we could refer to the work by Fard and Ragan (2017), which shapes healthy and diseased states by using networks of multi-omic representations.

However, to advance this segment of research, we need a source of data on neurochemistry inflammation that can be translated into matrices.

Another issue to be addressed is stability, and more precisely, how to keep a brain’s state within the subspace “healthy”, allowing only fluctuations within a certain range. In particular, we have assumed, for what concerns the subspace of healthy brain states, a basin of attraction of brain states. The stability with respect to such a basin characterises a healthy brain, whose states are not pathological, or do not involve any pathological state. A process of complete healing from a neuropsychiatric disease involves the progressive disappearance of pathological states, and a permanence of the brain, after a certain time point, within the basin of attraction of healthy states. However, the precise definition of such a basin requires further experimental investigation.

Author Contributions M.M. had the initial idea, performed the computations, wrote the article. P.R., N.M., and P.F. discussed and helped improve the idea, and carefully revised the article. N.M. supervised the research.

Funding Open access funding provided by Consiglio Nazionale Delle Ricerche (CNR) within the CRUI-CARE Agreement. This paper was developed within the project funded by Next Generation EU – “Age-It – Ageing well in an ageing society” project (PE0000015), National Recovery and Resilience Plan (NRRP) – PE8 – Mission 4, C2, Intervention 1.3, CUP B83C22004880006.

The research by P.F. was supported by the European Union within the REFRESH project – Research Excellence For Region Sustainability and High-tech Industries ID No. CZ.10.03.01/00/22 003/0000048 of the European Just Transition Fund.

Data Availability All information are available from the article itself.

Code Availability The code to compute the K -operator, given DICOM files as input for two different time points, can be accessed at https://github.com/medusamedusa/K_operator_parkinson (DOI 10.5281/zen-

odo.14162649), concerning in particular patient B, #100006, atlas AAL3, and https://github.com/medusamedusa/AAL3_K-operator_AD; and the detailed discussion of the definition of the operator is proposed in Mannone et al. (2024c).

The code to compute the brain space can be accessed at <https://github.com/medusamedusa/BrainSpaces> and <https://codeberg.org/medusamedusa/BrainSpaces.git>, DOI: <https://doi.org/10.5281/zenodo.15302779>.

Declarations

Competing Interests The authors declare no competing interests.

Open Access This article is licensed under a Creative Commons Attribution 4.0 International License, which permits use, sharing, adaptation, distribution and reproduction in any medium or format, as long as you give appropriate credit to the original author(s) and the source, provide a link to the Creative Commons licence, and indicate if changes were made. The images or other third party material in this article are included in the article's Creative Commons licence, unless indicated otherwise in a credit line to the material. If material is not included in the article's Creative Commons licence and your intended use is not permitted by statutory regulation or exceeds the permitted use, you will need to obtain permission directly from the copyright holder. To view a copy of this licence, visit <http://creativecommons.org/licenses/by/4.0/>.

References

- Battiston, F., Cencetti, G., Iacopini, I., Latora, V., Lucas, M., Patania, A., Young, J. G., & Petri, G. (2020). Networks beyond pairwise interactions: Structure and dynamics. *Physics Reports*, *874*, 1–192.
- Bergamino, M., Keeling, E. G., Ray, N. J., Macerollo, A., Silverdale, M., Stokes, A. M. (2023). Structural connectivity and brain network analyses in Parkinson's disease: A cross-sectional and longitudinal study. *Frontiers in Neurology*, *14*, 1137780.
- Blandini, F., Nappi, G., Tassorelli, C., & Martignoni, E. (2000). Functional changes of the basal ganglia circuitry in Parkinson's disease. *Progress in Neurobiology*, *62*(1), 63–88.
- Buxton, R.B. (2013). The physics of functional magnetic resonance imaging (fMRI). *Reports on Progress in Physics*, *76*(9).
- Buzsáki, G., & Llinás, R. (2017). Space and time in the brain. *Science*, *358*, 482–485. <https://doi.org/10.1126/science.aan8869>
- Davis, K. L., Kahn, R. S., Ko, G., & Davidson, M. (1991). Dopamine in schizophrenia: a review and reconceptualization. *The American Journal of Psychiatry*, *148*(11), 1474–86. <https://doi.org/10.1176/ajp.148.11.1474>
- Fard, T.A., Ragan, M.A. (2017). Modeling the attractor landscape of disease progression: a network-based approach. *Frontiers in Genetics*, *8*(48). <https://doi.org/10.3389/fgene.2017.00048>
- Fathian, A., Jamali, Y., Raoufy, M., et al. (2022). The trend of disruption in the functional brain network topology of Alzheimer's disease. *Scientific Reports*, *12*, 14998. <https://doi.org/10.1038/s41598-022-18987-y>
- Hagmann, P. (2005). From diffusion MRI to brain connectomics (Thesis). Phd thesis, EPFL, Lausanne. <https://doi.org/10.5075/epfl-thesis-3230>
- Kennedy, D. et al. (2023). HarvardOxford cort maxprob thr25 2mm. <https://fsl.fmrib.ox.ac.uk/fsl/fslwiki/Atlases>
- Li, Q., Seraji, M., Calhoun, V.D., Iraj, A. (2024). Complexity Measures of Psychotic Brain Activity in the fMRI Signal. In: 2024 IEEE southwest symposium on image analysis and interpretation (SSIAI), pp. 9–12. <https://doi.org/10.1109/SSIAI59505.2024.10508702>
- Mannone, M., Fazio, P., Ribino, P., & Marwan, N. (2024a). On disease and healing: a theoretical sketch. *Frontiers in Applied Mathematics and Statistics*, *10*. <https://doi.org/10.3389/fams.2024.1468556>
- Mannone, M., Fazio, P., Marwan, N. (2024b). Modeling a neurological disorder as the result of an operator acting on the brain: a first sketch based on network channel modeling. *Chaos*, *34*(5). <https://doi.org/10.1063/5.0199988>
- Mannone, M., Fazio, P., Kurths, J., Ribino, P., & Marwan, N. (2024c). A brain network operator for modeling disease: a first data-based application for parkinson's disease. *European Physical Journal, Special Topics*. <https://doi.org/10.1140/epjs/s11734-024-01345-6>
- Mannone, M., Marwan, N., Fazio, P., & Ribino, P. (2025). Limbic and cerebellar effects in Alzheimer-Perusini's disease: A physics-inspired approach. *Biomedical Signal Processing and Control*, *103*, 107355.
- Morris, L. A., et al. (2023). Altered nucleus accumbens functional connectivity precedes apathy in Parkinson's disease. *Brain*, *3*(146), 2739–2752.
- Mosley, P. E., Robinson, G. A. (2023). Functional network reorganization precedes apathy in Parkinson's disease: a neural marker of risk?. *Brain*, *146*(7), 2661–2662 <https://doi.org/10.1093/brain/awad180>
- Newman, M. E. J. (2003). The Structure and Function of Complex Networks. *SIAM Review*, *45*(2), 167–256.
- Olszewska, A., Gaca, M., Herman, A., Jednoróg, K., Marchewka, A. (2021). How musical training shapes the adult brain: predispositions and neuroplasticity. *Frontiers in Neuroscience*, *15*, 630829. <https://doi.org/10.3389/fnins.2021.630829>
- O'Shea, I. M., Popal, H. S., Olson, I. R., et al. (2022). Distinct alterations in cerebellar connectivity with substantia nigra and ventral tegmental area in Parkinson's disease. *Scientific Reports*, *12*, 3289.
- Reichl, L.E. (1998). *A Modern Course in Statistical Physics* (Wiley-VCH)
- Rolls, E. T., Huang, C. C., Lin, C. P., Feng, J., & Joliot, M. (2020). Automated anatomical labelling atlas 3. *Neuroimage*, *206*, Article 116189.
- Sacks, O. (2007). *Musophilia: Tales of Music and the Brain*. Knopf, New York: Alfred A. Knopf.
- Sang, L., Zhang, J., Wang, L., Zhang, Y., Li, P., Wang, J., & Qiu, M. (2015). Alteration of brain functional networks in early-stage Parkinson's disease: a resting-state fMRI study. *PLoS one*, *10*(10), Article e0141815.
- Schummer, G. (2009). The Disconnection Syndrome. Biofeedback. <https://web.archive.org/web/20150907181212/http://www.resourcenter.net/images/AAPB/Files/Biofeedback/2008/biof-36-04-157-162.pdf>
- Seeley, W. W. (2017). Mapping neurodegenerative disease onset and progression. *Cold Spring Harbor Perspectives in Biology*, *9*, Article a023622.
- Smith, R. E., Tournier, J. D., Calamante, F., & A. (2012). Connely, Anatomically-constrained tractography: Improved diffusion MRI streamlines tractography through effective use of anatomical information. *NeuroImage*, *62*(3), 1924–1938. <https://doi.org/10.1016/j.neuroimage.2012.06.005>. <https://www.sciencedirect.com/science/article/pii/S1053811912005824>
- Sporns, O., Tononi, G., & Kötter, R. (2005). The human connectome: A structural description of the human brain. *PLoS Computational Biology*, *1*(4), Article e42. <https://doi.org/10.1371/journal.pcbi.0010042>
- Staff, H. (2022). Areas of the brain affected by Alzheimer's and other dementias. <https://myhealth.alberta.ca/Health/pages/conditions.aspx?hwid=tp12408&lang=en-ca#:~:text=The%20damaged%20areas%20of%20the,the%20parietal%20lobe%20affects%20language>
- Tzourio-Mazoyer, N., Landeau, B., Papathanassiou, D., Crivello, F., Étard, O., Delcroix, N., Mazoyer, B., Joliot, M. (2002). Automated

- Anatomical Labeling of Activations in SPM Using a Macroscopic Anatomical Parcellation of the MNI MRI Single-Subject Brain. *Neuroimage*, 15, 273–289. <http://dx.doi.org/10.1006/nimg.2001.0978>
- van den Heuvel, M. P., Mandl, R. C., Stam, C. J., Kahn, R. S., & Pol, H. E. H. (2010). Aberrant frontal and temporal complex network structure in schizophrenia: a graph theoretical analysis. *The Journal of Neuroscience*, 30(47), 15915–15926.
- van den Heuvel, M. P., & Sporns, O. (2013). Network Hubs in the Human Brain. *Trends in Cognitive Sciences*, 12(12), 683–696.
- van Hooijdonk, C. F., van der Pluijm, M., Bosch, I., van Amelsvoort, T. A., Booij, J., de Haan, L., Selten, J. P., & van de Giessen, E. (2023). The substantia nigra in the pathology of schizophrenia: A review on post-mortem and molecular imaging findings. *European Neuropsychopharmacology*, 68, 57–77. <https://doi.org/10.1016/j.euroneuro.2022.12.008>. <https://www.sciencedirect.com/science/article/pii/S0924977X22009191>
- Varoquaux, G., Gramfort, A., Pedregosa, F., Michel, V., Thirion B. (2011). Multisubject dictionary learning to segment an atlas of brain spontaneous activity. In: Information processing in medical imaging (IPMI 2011), ed. by G. Székely, H. Hahn (Springer, Cham), pp. 562–573

Publisher's Note Springer Nature remains neutral with regard to jurisdictional claims in published maps and institutional affiliations.